

A SEDIMENT TRANSPORT EQUATION FOR INTERRILL OVERLAND FLOW ON ROUGH SURFACES

ATHOL D. ABRAHAMS,^{1,*} GARY LI,² CHITRA KRISHNAN³ AND JOSEPH F. ATKINSON⁴

¹ Department of Geography, State University of New York at Buffalo, Buffalo, New York 14261, USA

² Department of Geography and Environmental Studies, California State University Hayward, California 94542, USA

³ Department of Applied Mechanics, Indian Institute of Technology, New Dehli 110 016, India

⁴ Department of Civil, Structural, and Environmental Engineering, State University of New York at Buffalo, Buffalo, New York 14260, USA

Received 20 March 2000; Revised 15 March 2001; Accepted 17 September 2001

ABSTRACT

A model for predicting the sediment transport capacity of turbulent interrill flow on rough surfaces is developed from 1295 flume experiments with flow depths ranging from 3.4 to 43.4 mm, flow velocities from 0.09 to 0.65 m s⁻¹, Reynolds numbers from 5000 to 26949, Froude numbers from 0.23 to 2.93, bed slopes from 2.7° to 10°, sediment diameters from 0.098 to 1.16 mm, volumetric sediment concentrations from 0.002 to 0.304, roughness concentrations from 0 to 0.57, roughness diameters from 1.0 to 91.3 mm, rainfall intensities from 0 to 159 mm h⁻¹, flow densities from 1002 to 1501 kg m⁻³, and flow kinematic viscosities from 0.913 to 2.556 × 10⁻⁶ m² s⁻¹. Stones, cylinders and miniature ornamental trees are used as roughness elements. Given the diverse shapes, sizes and concentrations of these elements, the transport model is likely to apply to a wide range of ground surface morphologies.

Using dimensional analysis, a total-load transport equation is developed for open-channel flows, and this equation is shown to apply to interrill flows both with and without rainfall. The equation indicates that the dimensionless sediment transport rate ϕ is a function of, and therefore can be predicted by, the dimensionless shear stress θ , its critical value θ_c , the resistance coefficient u/u_* , the inertial settling velocity of the sediment w_i , the roughness concentration C_r , and the roughness diameter D_r . The model has the form

$$\phi = a\theta^{1.5} \left(1 - \frac{\theta_c}{\theta}\right)^{3.4} \left(\frac{u}{u_*}\right)^c \left(\frac{w_i}{u_*}\right)^{-0.5}$$

where $\log a = -0.42 C_r/D_r^{0.20}$ and $c = 1 + 0.42 C_r/D_r^{0.20}$. Testing reveals that the model gives good unbiased predictions of ϕ in flows with sediment concentrations less than 0.20. Flows with higher concentrations appear to be hyperconcentrated and to have sediment transport rates higher than those predicted by the model. Copyright © 2001 John Wiley & Sons, Ltd.

KEY WORDS: sediment transport; bed load; total load; soil erosion; interrill flow; overland flow; hillslopes

INTRODUCTION

The sediment transport capacity of overland flow is the maximum sediment transport rate of the flow. Virtually all physically based soil erosion models contain an equation for predicting transport capacity because transport capacity plays a key role in determining (1) whether a sediment-laden flow experiences erosion or deposition and (2) the net rates at which these processes occur (e.g., Foster *et al.*, 1995; Smith *et al.*, 1995; Morgan *et al.*, 1998). The sediment transport capacity therefore is a property of fundamental importance, and its accurate prediction is essential if soil erosion models are to represent effectively the processes of detachment, transport and deposition.

* Correspondence to: A. D. Abrahams, Department of Geography, State University of New York at Buffalo, Buffalo, NY 14261, USA. E-mail: abrahams@geog.buffalo.edu

Contract/grant sponsor: National Science Foundation; Contract/grant number: SES-9213378 and DEB-9411971.

The formulation of a suitable equation for predicting the sediment transport capacity of interrill flow has been complicated by the fact that hillslope surfaces, whether natural or disturbed by agriculture, are hydraulically very rough (in the sense that roughness elements such as microtopographic protuberances, stones, and plant stems, leaves and litter typically disturb the water surface and often protrude through it), and this roughness substantially reduces the transport capacity (Govers and Rauws, 1986; Abrahams and Parsons, 1994; Abrahams *et al.*, 1998, 2000). In river hydraulics the traditional way of estimating the reduction in transport capacity due to the form drag imparted by roughness elements is to partition the total shear stress into grain shear stress and form shear stress and then predict transport capacity using the former. However, this approach does not work in interrill flow (Abrahams and Parsons, 1994; Atkinson *et al.*, 2000) because eddies produced by the roughness elements occur so close to the bed that they become involved in the transport process. Thus, actual sediment transport rates are less than those predicted by total shear stress but more than those predicted by grain shear stress. However, it is difficult to be more precise.

Another approach to predicting the transport capacity of rill and interrill flow was suggested by Govers (1992). He proposed predicting transport capacity using hydraulic variables that implicitly account for the effect of surface roughness. This approach is based on the hypothesis that, inasmuch as surface roughness affects flow hydraulics which, in turn, determine transport capacity, there may be one or more hydraulic variables that capture the effect of surface roughness on transport capacity sufficiently well for good predictions of transport capacity to be achieved using these variables. We investigated this hypothesis by performing 1506 flume experiments on interrill overland flows in which discharge, slope, water temperature, rainfall intensity, and roughness size, shape and concentration varied widely (Abrahams *et al.*, 1998). Multiple regression analysis revealed that almost 90 per cent of the variance in transport capacity could be accounted for by excess flow power and flow depth. Evidently, these two hydraulic variables, when used together, largely capture the effect of surface roughness on transport capacity.

Although we showed that the transport capacity of interrill flow on rough surfaces could be well predicted by hydraulic variables alone, we were unable to develop an equation for this purpose because our flume experiments were all performed with a single sediment size. We therefore have conducted a further set of experiments on three additional sand sizes. The data from these experiments are combined with those from the previous experiments, and the combined data set is used to develop and then test an equation for predicting the sediment transport capacity of interrill flow on rough surfaces.

Although there are parts of this paper wherein a distinction is drawn between plane and rough beds, in some analyses and discussions these bed types are lumped together and collectively referred to as 'rough'. In these situations the plane beds are viewed as end members of the bed roughness continuum. The terms bed roughness, surface roughness and boundary roughness are used interchangeably and encompass both grain resistance and form resistance in its broadest sense to include wave resistance (Abrahams *et al.*, 1992; Abrahams and Parsons, 1994; Hirsch, 1996; Lawrence, 2000). It is emphasized, however, that, except on plane or almost-plane beds, grain resistance is a negligible proportion of the total flow resistance, which is dominated by form resistance.

Finally, in what follows we refer to the paper by Abrahams *et al.* (1998) as 'our earlier paper'.

SET-UP AND METHODS

The present experiments were conducted in two flumes but, as these flumes were almost identical (the principal difference being that water was recirculated in one but not in the other), they will be treated as if they were one. Because the flume set-up and methods were described in our earlier paper, only a summary is given here. Greater detail is provided where there are departures from the previous methods.

The flume was 5.2 m long and 0.4 m wide, and consisted of two parts: a 3.6-m-long lower section, which had a sandy bed, and a steeper 1.6-m-long upper section, which had a smooth aluminum floor. During the experiments the slope β of the lower section was varied between 2.7° and 10° . The effect of slope on sediment transport is customarily represented by either $\tan \beta$ or $\sin \beta$. This practice, however, neglects the fact that as β increases, the downslope component of gravity increases, facilitating the entrainment and transport of bed sediments. Thus, sediment transport rates increase at an increasing rate as β approaches the angle of repose α ,

which generally is taken to be about 32° (so $\tan \alpha = 0.63$). When $\beta = \alpha$, the bed fails and the grains move downslope en masse.

Bagnold (1966, 1973) provided a more formal explanation for this phenomenon. He reasoned that the tangential fluid shear stress $T = W' \cos \beta \tan \alpha$ necessary to sustain bed sediments in transport is reduced by the portion of the shear stress $W' \sin \beta$ applied to the immersed load W' by gravity. This portion increases with β until the bed fails when $\beta = \alpha$ and the fluid shear stress required to sustain sediment transport $T - W' \sin \beta = W' \cos \beta (\tan \alpha - \tan \beta) = 0$. Given that β ranges up to 10° in the present experiments, $W' \sin \beta$ is expected to have a significant impact on sediment transport rates. The appropriate measure of slope S in these circumstances is obtained by multiplying the conventional measure $\sin \beta$ by the factor $\tan \alpha / [\cos \beta (\tan \alpha - \tan \beta)]$, which varies from 1 to ∞ as β varies from 0 to α . Note that this factor is the inverse of the Schoklitsch (1914) slope factor discussed by van Rijn (1993, pp. 4.11 and 7.29).

Sand was delivered to the upper section of the flume by a vibrating hopper. On the steep aluminum bed the sand was easily entrained and transported to the lower section of the flume. Four well-sorted sands with median diameters D of 0.098, 0.25, 0.74 and 1.16 mm and standard deviations $(D_{84}/D_{16})^{0.5}$ of 1.17, 1.10, 1.08 and 1.19, respectively, were used in the experiments. These diameters cover the full range of sand sizes from very fine to very coarse (e.g. Leeder, 1982, p. 36). Simulated rainfall was applied in some experiments at target intensities of 54, 108 and 162 mm h^{-1} . Actual intensities, which were measured by eight rain gauges, varied slightly. At the target intensities, median drop sizes were 1.6, 2.0 and 2.4 mm and total kinetic energies were 0.24, 0.65 and 1.19 $\text{J m}^{-2} \text{s}^{-1}$, which were equal to 48, 68 and 85 per cent of the energies of natural rainstorms at the same intensities (Kinnell, 1973).

Water entered the upper end of the flume by overflowing from a head tank. The inflow rate was measured by a flow meter located on the inlet pipe to the head tank. The volumetric water discharge Q_w ($\text{m}^3 \text{s}^{-1}$) from the flume was equal to the inflow plus any simulated rainfall. The volumetric sediment discharge Q_s ($\text{m}^3 \text{s}^{-1}$) was determined by sampling the water-sediment mixture leaving the flume, weighing the water and sediment in the each sample, and converting the weights to volumes by multiplying by the water and sediment densities $\rho = 1000 \text{ kg m}^{-3}$ and $\rho_s = 2650 \text{ kg m}^{-3}$, respectively. The volumetric sediment concentration C was then obtained from

$$C = Q_s / (Q_w + Q_s) \quad (1)$$

and the volumetric sediment transport rate per unit width q_s ($\text{m}^{-2} \text{s}^{-1}$) from

$$q_s = Q_s / w \quad (2)$$

where

$$w = W(1 - C_r) \quad (3)$$

is the flow width (m), W the flume width (m) and C_r is the concentration of roughness elements defined as the proportion of the surface covered by these elements. Flow width rather than flume width is used to calculate q_s because, when the roughness elements protrude through the flow, as they do here, sediment transport is confined to the spaces between the elements. As a result, the transport capacity per unit flow width is higher (in response to the higher flow depth and shear stress) than if the transport capacity had been calculated per unit flume width. Likewise, flow width rather than flume width is used to compute flow depth from measurements of flow discharge and velocity. The mean flow velocity u (m s^{-1}) is determined by a salt-tracing technique described by Li and Abrahams (1997). The mean flow depth h (m) is then computed by dividing the bulk flow discharge ($\text{m}^3 \text{s}^{-1}$)

$$Q = Q_w + Q_s \quad (4)$$

by uw .

The lower section of the flume is divided into a 2.6-m-long test section and a 1-m-long approach section. Dowling rods placed across the flume at the upper end of the approach section (i.e. at the break in slope

between the steeper upper and gentler lower sections of the flume) reduce the flow velocity to a value close to that in the test section. Consequently, only a modest adjustment is needed for the flow to become fully developed, and this adjustment is easily achieved within the approach section irrespective of whether the bed is plane or rough.

The approach section also serves as a buffer or store of sediment, which aggrades or degrades when the supply from the hopper exceeds or is exceeded by the transport capacity of the flow. By adjusting the sediment feed rate, a uniform depth of sand is maintained in the approach section, and the flow transports sand at capacity through the test section. During experiments without rainfall both Q_w and Q_s are constant down flume. In contrast, during experiments with rainfall, Q_w increases but Q_s remains constant down flume. An increase in Q_s is possible only if the flow scours the bed. As there was no evidence of scouring, it is inferred that subtle adjustments in one or more other variables, such as hydraulic gradient, compensate for the down-flume increase in Q_w , thereby enabling Q_s to remain constant.

Irrespective of whether sediment is transported as suspended load or bed load, the rate of transport is influenced by the concentration of sediment particles in the flow. In deep open-channel flows, the bed load is confined to a thin layer close to the bed. Settling velocities and the density and viscosity of the fluid–grain mixture therefore are a function of the suspended sediment concentration. In interrill flow, however, the bed load is distributed over most of the flow depth. Consequently, the volumetric concentration C of the combined bed load and suspended load is used to calculate the density ρ (kg m^{-3}) and kinematic viscosity ν ($\text{m}^2 \text{s}^{-1}$) of the flow

$$\rho = \rho_s C + \rho_w (1 - C) \quad (5)$$

$$\nu = \mu / \rho \quad (6)$$

where ρ_w is the density of water (kg m^{-3}). The dynamic viscosity μ ($\text{kg m}^{-1} \text{s}^{-1}$) of the water–sediment mixture is estimated from (Coussot, 1997, p. 47)

$$\mu = \mu_w \left[1 + \frac{0.75}{(0.605/C) - 1} \right]^2 \quad (7)$$

where μ_w is the dynamic viscosity of the water ($\text{kg m}^{-1} \text{s}^{-1}$).

Because the mechanics of sediment entrainment and transport in laminar interrill flow are different from those in turbulent flow (Govers, 1987; Li and Abrahams, 1999), this study is confined to turbulent flow. The boundary between laminar and turbulent interrill flow has not been studied thoroughly and so it is not well understood. Savat (1980) undertook several hundred flume experiments involving supercritical interrill flows. The graphs of friction factor $f = 8ghS/u^2$ against flow Reynolds number $Re = 4uh/\nu$ for these experiments all displayed inflections at about $Re = 2440$. Savat therefore took this value of Re to be the boundary between laminar and turbulent interrill flows. However, other studies (e.g. Straub, 1939; Owen, 1954; Woo and Brater, 1961; Dunne and Dietrich, 1980) have indicated that in subcritical interrill flows the value of Re at the boundary is both higher and more variable than in the supercritical flows of Savat (1980).

Measurements of velocity fluctuations using hot-film anemometry support the latter conclusion. Data from three subcritical interrill flows are presented in Figure 1. In Figure 1a ($Re = 551$) the flow is wholly laminar; in Figure 1c ($Re = 5083$) it is fully turbulent, although only barely so; and in Figure 1b ($Re = 2622$) it is both laminar and turbulent. Evidently, the onset of fully turbulent flow occurs where $2622 < Re < 5083$. A criterion of $Re \geq 5000$ therefore was adopted as a requirement for an experiment to be included in the present study. Experiments with $Re < 5000$ were excluded. Flows disturbed by rainfall and large-scale roughness elements probably become fully turbulent at lower Re values. In the absence of any quantitative evidence on the effect of these disturbances, however, it was decided to err on the side of caution and apply the criterion of $Re \geq 5000$ to all experiments.

In our earlier paper we analysed 1506 experiments with $Re > 2000$ and $D = 0.74$ mm. With the goal of developing a general sediment transport equation for sand-sized sediment, 344 new experiments were

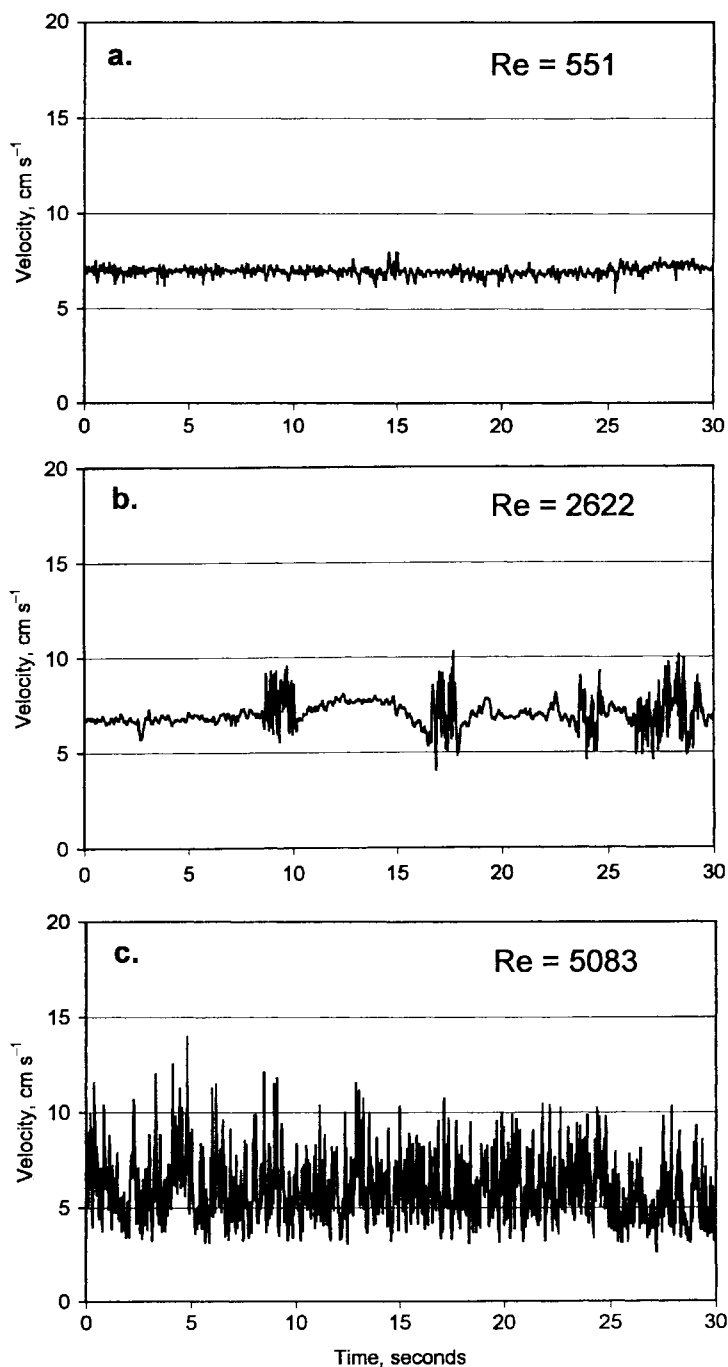


Figure 1. Graphs of flow velocity against time measured at a rate of 400 Hz at a distance of $0.37h$ from the bed. Re is the flow Reynolds number defined in the text

completed using three other sand sizes. The original 1506 experiments represent a wide range of conditions (i.e. Reynolds number, bed slope, fluid viscosity, and roughness size, shape and concentration), much wider than for any other sand size. Thus, the sample of experiments to be analysed here should include more experiments with the 0.74-mm sand than with any other sand size. However, there were so many experiments with the

0.74-mm sand that if all were included, they would bias the results. The original sample of 1506 experiments was therefore divided into two groups. By the simple expedient of selecting every third experiment in the spreadsheets, a group of 501 experiments was identified. Of these original experiments, 195 were discarded because Re was less than 5000. The remaining 306 experiments were combined with the 343 new experiments to form sample A. This sample of 649 experiments was then assigned to model development.

The second group of 1005 experiments minus 359 experiments for which Re was less than 5000 was designated sample B. This sample of 646 experiments was reserved for model testing. Obviously, sample B, which contains only one sand size and is drawn from the same population as about half of sample A, is less than ideal as a test sample. Still, it represents a wide range of flow properties and surface roughnesses, and so it provides some basis for evaluating the derived transport equation.

The experiments in samples A and B were grouped into the same six series as we used in our earlier paper (Table I). The first and second series were conducted on plane beds with no roughness elements. During the second series simulated rainfall was applied at the target intensities specified above. The third series used cylinders as roughness elements. Four roughness sizes (i.e. cylinder diameters) D_r (m) between 0.95 and 8.9 cm were used in this series at concentrations C_r ranging from 0.04 to 0.35. The cylinders were arranged into random patterns and were sufficiently tall that they were never inundated by the flow. Simulated rainfall was eschewed because all but the smallest cylinders were hollow and would have filled with rain water.

Simulated rainfall was applied in the fifth series but not in the fourth. In both series the flume bed was covered with three groups of stones. The stones in these groups were similar in shape and roundness but different in size (Table II). Inasmuch as the stones were placed randomly in the flume with their a - b planes parallel to the bed, D_r was represented by $(a + b)/2$. The median values of D_r for the three groups was 28.0, 45.5, and 91.3 mm, and C_r varied over the range of 0.04 to 0.57. The c axes of the stones in the three groups had median lengths of 16.0, 25.0 and 53.5 mm. The stones were partly buried in the sandy bed, with those in the second and third groups (i.e. the largest stones) being buried by about 10 mm and those in the first group (i.e. smallest stones) by about 4 mm. Nevertheless, many, if not most, of the stones in the third group were inundated by the highest discharges. When inundation occurs, w is no longer given by Equation 3, and h , which is calculated using this equation, will be in error. This is a source of concern both in the present experiments and in applications of sediment transport models to rough surfaces where h is calculated assuming a constant w . The variation in w may be modelled from a knowledge of (or assumptions about) the surface morphology (e.g. Dunne *et al.*, 1991; Bunte and Poesen, 1994; Kirkby *et al.*, 1998) but, given the variable heights of the stones and the absence of any information on these heights, no effort was made to incorporate the variation in w with Q into the present analysis. Instead, a constant value of C_r was determined for each surface assuming no inundation, w was estimated using Equation 3, and h obtained from $h = Q/wu$.

In the series-6 experiments, miniature ornamental Christmas (i.e. conifer-like) trees were used as roughness elements in order to provide a type of roughness quite different from cylinders and stones and more like grass, plant stems and litter. Given that the flow passes through the trees, the roughness size was set equal to the thickness of the branches and leaves, which was 1 mm. The permeable nature of the trees, however, made calculation of the roughness concentration problematic, as the actual concentration C_r was less than the apparent concentration C_a when viewed from above. In order to estimate C_r from measurements of C_a a relationship was developed between these two variables in the following way. A layer of sand was placed in a 1-m² pan, and miniature trees were planted in the sand with $C_a = 0.62$. The sand surface was then flooded until the water reached the lip of an overflow about 1.5 cm above the sand bed. The trees were then removed three or four at a time. After each group was removed C_a was measured, and the volume occupied by the trees below the water surface was determined by measuring the volume of water that had to be added to the pan to raise the water level back to the lip. Knowing the change in volume associated with each change in C_a , it was possible to calculate the relationship between C_r and C_a , which was found to be $C_r = 0.60C_a$.

DIMENSIONAL ANALYSIS

Dimensional analysis begins with the basic independent variables that characterize a system and arranges them into a parsimonious functional relationship with coefficients that are then determined by statistical analysis of

Table I. Summary of experimental data

	Series					
	1	2	3	4	5	6
Roughness type	Plane bed	Plane bed	Cylinders	Stones	Stones	Miniature trees
Number of experiments	61	55	559	260	277	83
Mean flow depth (m)	0.0034–0.0105	0.0034–0.0106	0.0049–0.0287	0.0042–0.0434	0.0055–0.0396	0.0065–0.0358
Mean flow velocity (m s ⁻¹)	0.216–0.653	0.235–0.588	0.129–0.433	0.120–0.422	0.138–0.505	0.091–0.323
Reynolds number	5042–13 018	5107–11 439	5000–19 061	5010–26 949	5012–21 914	5032–19 859
Froude number	0.74–2.93	0.84–2.82	0.29–1.91	0.23–2.04	0.28–1.88	0.16–1.27
Slope (degrees)	2.7, 5.5, 10	2.7, 5.5, 10	2.7, 5.5, 10	2.7, 5.5	2.7, 5.5, 10	2.7, 5.5, 10
Sediment size (mm)	0.25, 0.74, 1.16	0.74, 1.16	0.098, 0.25, 0.74, 1.16	0.098, 0.74, 1.16	0.098, 0.74, 1.16	0.74
Sediment concentration	0.00937–0.16199	0.00968–0.06196	0.00211–0.18097	0.00473–0.30364	0.00432–0.27658	0.00109–0.10384
Roughness concentration	0	0	0.04–0.35	0.04–0.57	0.08–0.57	0.10–0.28
Roughness diameter (mm)	0	0	9.5, 21.6, 31.7, 89.0	28.0, 45.5, 91.3	28.0, 45.5, 91.3	1.0
Rainfall intensity (mm h ⁻¹)	0	53–144	0	0	53–152	0
Density of fluid–grain mixture (kg m ⁻³)	1015.5–1264.8	1016.0–1102.3	1003.5–1297.5	1007.8–1500.9	1007.1–1454.6	1001.8–1154.4
Kinematic viscosity of fluid–grain mixture (×10 ⁻⁶ m ² s ⁻¹)	1.054–1.535	1.053–1.529	1.017–1.652	0.971–2.556	0.913–2.253	1.102–1.329

Table II. Properties of the stone roughness elements

Group	Median length				Mean Corey shape factor	Modal Powers roundness index
	<i>a</i> axis (cm)	<i>b</i> axis (cm)	<i>c</i> axis (cm)	(<i>a</i> + <i>b</i>)/ <i>c</i> (cm)		
1	3.20	2.40	1.60	2.80	0.605	5
2	5.20	3.90	2.50	4.55	0.566	5
3	10.80	7.46	5.35	9.13	0.596	5

experimental data. The basic variables involved in the transport of cohesionless grains over a plane bed by a fluid flow with a free surface are contained in the functional relationship

$$\varphi(\rho, \rho_s, \mu, h, u, g, S, D, q_s) = 0 \quad (8)$$

Utilizing the rule that any basic variable may be replaced by any dependent combination in which it occurs (Yalin, 1972, p. 57), we replaced g in Equation 8 by $\gamma_s = g(\rho_s - \rho)$ and ρ_s by $(\rho_s - \rho)$. Yalin (1972, p. 58) argued that S should be replaced by u^* , as the role of slope is merely to establish the gravity component gS of the flow-generating force ρu^{*2} where $u^* = (gsh)^{0.5}$ is the shear velocity. This may be true on gentle slopes, but it is not on steep ones. This can be seen in Smart's (1984) and Rickenmann's (1991) flume experiments, which were conducted on slopes up to 11.3° ($\tan \beta = 0.20$). In these experiments $q_s \propto u^{*2} \tan^{0.6} \beta$ (Smart, 1984, equations 7 and 8) and $q_s \propto u^{*1.9} \tan^{0.55} \beta$ (Rickenmann, 1991, equation 11). These relationships leave little doubt that $\tan \beta$ influences q_s independently of u^* and, consequently, that both S and u^* should appear in the functional relationship. Equation 8 therefore becomes

$$\varphi(\rho, \mu, h, u, \rho_s - \rho, \gamma_s, u^*, S, D, q_s) = 0 \quad (9)$$

No rainfall variable appears in this equation because, as we showed in our earlier paper, rainfall has little or no effect on the sediment transport capacity of turbulent interrill flows. Additional data presented below corroborate this finding.

Selecting D , ρ and u^* as the repeating variables and applying the Π -theorem leads to the functional relationship

$$q_s/(Du^*) = \varphi_3(Re^*, \theta, u/u^*, w_i/u^*) \quad (10)$$

where $Re^* = u^* D/\nu$ is the boundary Reynolds number, $w_i/u^* = (Sh/\Delta D)^{-0.5}$ is the dimensionless sediment fall velocity, $w_i = (g\Delta D)^{0.5}$ is the inertial fall velocity, and $\Delta = (\rho_s - \rho)/\rho$ is the relative sediment density. The battery of dimensionless variables includes Re^* because it is related to the hydrodynamic character of the bed and, hence, to the critical value of θ , denoted by the subscript c , at which the bed sediments begin to move. In this study θ_c was estimated using the relationship between θ_c and $\Xi^{0.5}$ developed by Yalin (1972, p. 82) and revised by Miller *et al.* (1977), where $\Xi^{0.5} = Re^*/\theta^{0.5}$. This estimate was corrected for the effect of the downslope component of gravity (Stevens *et al.*, 1976; Smart, 1984; Chiew and Parker, 1994) by dividing θ_c by the factor $\tan \alpha/[\cos \beta(\tan \alpha - \tan \beta)]$ discussed above. The corrected value of θ_c was then subtracted from θ to give the excess dimensionless shear stress $\theta - \theta_c$. Lastly, this quantity was substituted for θ in the functional relationship, giving

$$q_s/(Du^*) = \varphi_4(\theta - \theta_c, u/u^*, w_i/u^*) \quad (11)$$

Note that w_i rather than the actual fall velocity w_f appears in Equation 11 because

$$\frac{w_f}{u^*} = \varphi_5 \left(\frac{Re^*}{\theta^{0.5}} \right) \frac{w_i}{u^*} \quad (12)$$

(Yalin, 1972, p. 72). This equation signifies that inasmuch as θ_c , and hence $Re^*/\theta^{0.5}$, are already in the functional relationship, w_i/u^* rather than w_f/u^* is the appropriate measure of settling velocity to include in the relationship, as the latter variable includes Re^*/θ_c (which is redundant and introduces noise), whereas the former does not.

Multiplying both sides of Equation 11 by $\theta^{0.5}$ yields

$$\phi = \varphi_6 \left[\theta^{0.5}, (\theta - \theta_c), \frac{u}{u^*}, \frac{w_i}{u^*} \right] \tag{13}$$

where

$$\phi = \frac{q_s}{(g\Delta D)^{0.5} D} = \left(\frac{q_s}{Du^*} \right) \theta^{0.5} \tag{14}$$

is the dimensionless sediment transport rate. In keeping with Abrahams and Gao's (in preparation) bed-load transport model

$$\phi_b = \theta^{1.5} \left(1 - \frac{\theta_c}{\theta} \right)^{3.4} \frac{u}{u^*} \tag{15}$$

where ϕ_b is the dimensionless bed-load transport rate, Equation 13 was modified by multiplying $\theta^{0.5}$ by θ and dividing $\theta - \theta_c$ by θ to give $\theta^{1.5}$ and $1 - (\theta_c/\theta)$, respectively. With these changes, the functional relationship expressed as a power product becomes

$$\phi = a\theta^{1.5} \left(1 - \frac{\theta_c}{\theta} \right)^b \left(\frac{u}{u^*} \right)^c \left(\frac{w_i}{u^*} \right)^d \tag{16}$$

For plane beds where $a = 1$, $b = 3.4$ and $c = 1$, it can be seen that ϕ is the product of ϕ_b (Equation 15) and $(w_i/u^*)^d$. It follows that $\phi_b/\phi = P_b = (w_i/u^*)^{-d}$, where P_b is the proportion of the total load that is bed load. In other words, in a graph of P_b against w_i/u^* on logarithmic axes, the slope of the relation is $-d$ (Figure 2).

The variation in d with w_i/u^* was investigated using data from 505 open-channel flows on plane beds obtained from the literature. The relevant publications are cited in Figure 4, and additional details are provided by Abrahams and Gao (in preparation). These flows were divided into seven classes on the basis of their w_i/u^* values. Equation 16 was then fitted separately to the data in each class using non-linear regression. As

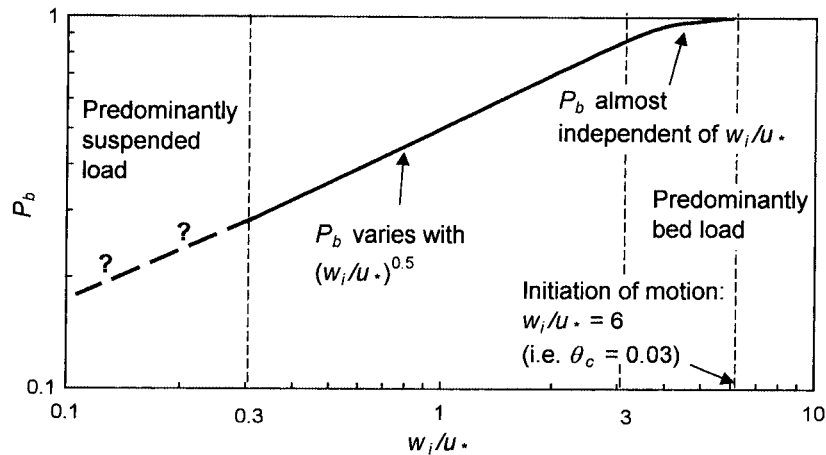


Figure 2. Graph of P_b against w_i/u^* showing the relationship between these two variables indicated by Figure 3

in Equation 15, the coefficients a , b and c were set equal to 1, 3.4, and 1, respectively, and the value of d was determined by the regression.

Figure 3 shows that d approximates 0 when $w_i/u_* \geq 3$ and -0.5 when $w_i/u_* < 3$. Setting d equal to these values, the total-load transport equation for plane beds is given by

$$\phi = \theta^{1.5} \left(1 - \frac{\theta_c}{\theta}\right)^{3.4} \frac{u}{u_*} \left(\frac{w_i}{u_*}\right)^d \quad (17)$$

where $d = 0$ when $w_i/u_* \geq 3$ and $d = -0.5$ when $w_i/u_* < 3$. Figure 4 indicates that Equation 17 is a good predictor of ϕ for open-channel flows on plane beds over seven orders of magnitude. That Equation 17 applies to such a wide range of conditions suggests that it also may apply to interrill flows.

COMPARISON OF OPEN-CHANNEL AND INTERRILL FLOWS

This suggestion was investigated by comparing the measured values of ϕ for the 66 plane-bed experiments in sample A with the values predicted by Equation 17. Figure 5a shows that there is excellent agreement between the measured and predicted values of ϕ . What is more, although 23 of the 66 experiments include rainfall, the rainfall and non-rainfall points intermingle in Figure 5a, suggesting that rainfall has little or no effect on the transport capacity of turbulent interrill flows. Thus it appears that on plane beds the transport capacity of both interrill and open-channel flows conform to and can be well predicted by Equation 17.

Figure 5b displays a plot of measured ϕ for the 649 experiments in sample A against the values of ϕ predicted for these experiments by Equation 17. This graph shows that Equation 17, which applies to plane beds, generally overpredicts ϕ for rough beds. In other words, surface roughness reduces ϕ below its value for an equivalent flow over a plane bed. The 10 flows that plot around the line of perfect agreement in the uppermost corner of the graph are an exception to this generalization. These flows are discussed at greater length below. First, however, we develop and then validate a model for predicting the transport capacity of interrill flow on rough surfaces.

MODEL DEVELOPMENT

The model for predicting the transport capacity of interrill flows is simply Equation 17 with variable a and c coefficients – that is,

$$\phi = a\theta^{1.5} \left(1 - \frac{\theta_c}{\theta}\right)^{3.4} \left(\frac{u}{u_*}\right)^c \left(\frac{w_i}{u_*}\right)^{-0.5} \quad (18)$$

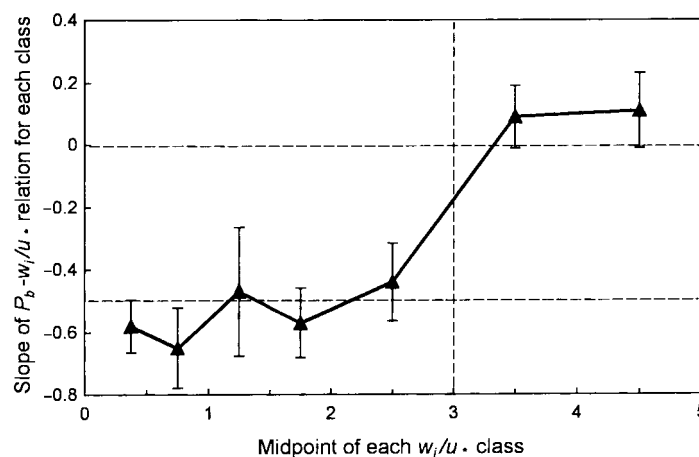


Figure 3. Graph of the slope of the $P_b - w_i/u_*$ relationship against w_i/u_* for 505 open-channel flows on plane beds. The error bars represent plus or minus two standard errors

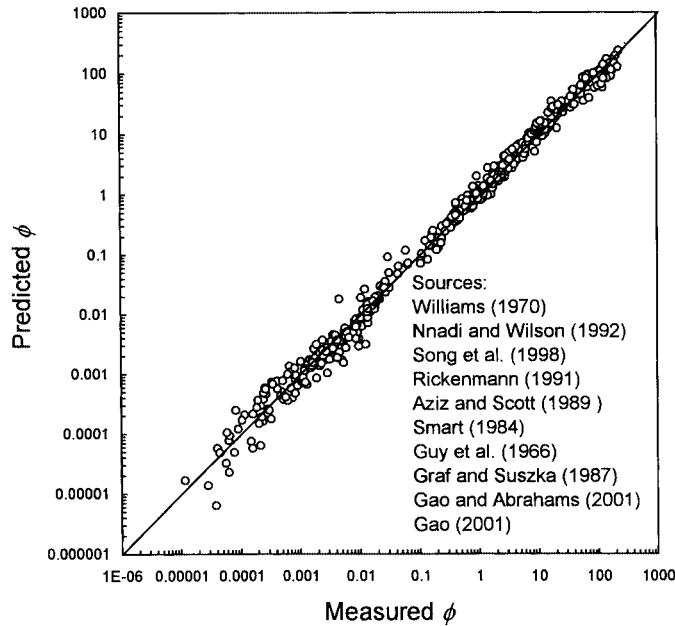


Figure 4. Graph of ϕ predicted by Equation 17 against ϕ of 505 open-channel flows on plane beds

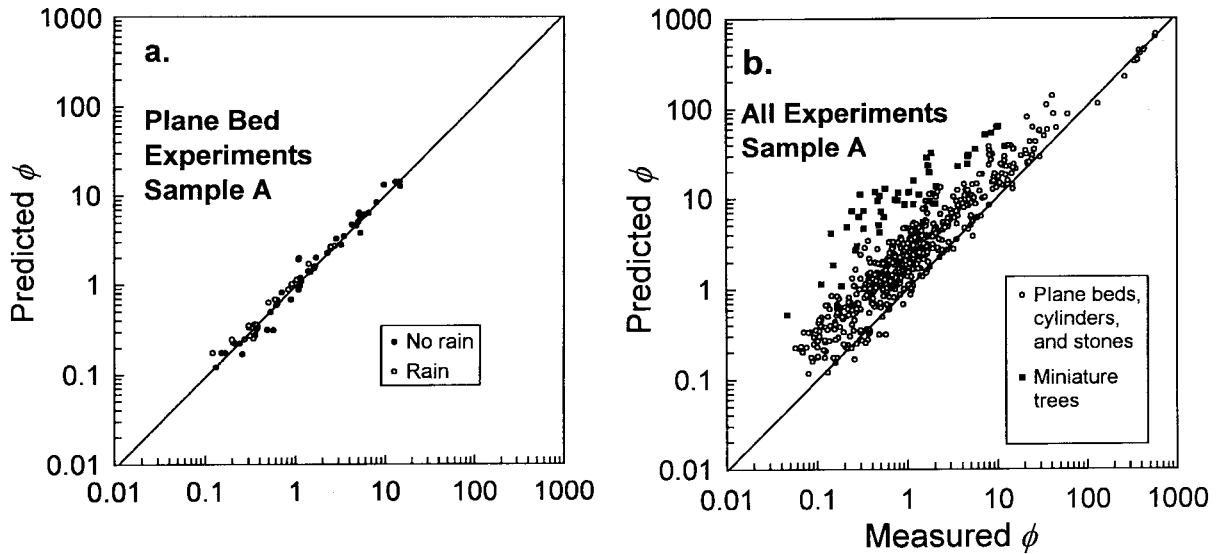


Figure 5. Graphs of ϕ predicted by Equation 17 against ϕ measured (a) for just the interrill flows over plane beds in sample A, and (b) for all the interrill flows in sample A

The exponent on w_i/u^* is fixed at -0.5 because w_i/u^* never exceeds 3 in samples A and B, suggesting that values greater than 3 may never occur or at least be quite rare in interrill flows. For flows on plane beds a and c both equal 1 (Equation 17). However, these coefficients progressively depart from 1 as surface roughness increases. Surface roughness reduces transport capacity through u/u^* because surface roughness increases flow resistance and decreases flow velocity, and u/u^* is the only measure of flow resistance in Equation 18.

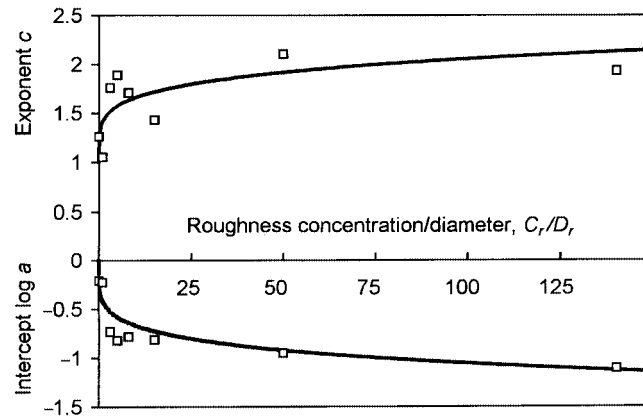


Figure 6. Graphs of the model parameters $\log a$ and c against roughness concentration divided by roughness diameter. The curves are Equations 19 and 20 with $j = 0.42$ and $k = 0.20$

The general form of the equations for predicting a and c was determined by dividing the 649 experiments in sample A into seven classes on the basis of their values of C_r/D_r . Equation 18 was then fitted separately to the data in each class. The ratio C_r/D_r is used here as an index of surface roughness on the basis of Abrahams *et al.*'s (2000) finding that C_r and D_r strongly influence the sediment transport capacity of turbulent interrill flow on stone-covered surfaces, with C_r being positively correlated and D_r negatively correlated with transport capacity. The computed values of $\log a$ and c for each class were graphed against C_r/D_r at the class mid-points (Figure 6). The graphs indicate that $\log a$ and c can be predicted by equations of the form

$$\log a = -jC_r/D_r^k \quad (19)$$

$$c = 1 + jC_r/D_r^k \quad (20)$$

Estimates of j and k were obtained by substituting Equations 19 and 20 into Equation 18 and then using non-linear regression to fit Equation 18 to the sample A data. This analysis yielded $j = 0.42$ and $k = 0.20$. Equations 19 and 20 with these estimates of j and k are depicted in Figure 6.

MODEL VALIDATION

Samples A and B

The ability of Equation 18 to predict the sediment transport capacity of interrill flow was tested by comparing predicted and measured values of ϕ for the flume experiments in samples A and B (Figure 7). With the exception of the uppermost 10 points in Figure 7a, the data for both samples plot close to and symmetrically around the line of perfect agreement. The agreement for sample B is particularly encouraging, as this sample was not used either to develop or to parameterize the model. A comparison of Figures 7a and b reveals that sample A has a larger range of ϕ than does sample B. This is because ϕ contains D in its definition (Equation 14) and sample A has a larger range of D ($0.098 \leq D \leq 1.16$ mm) than does sample B ($D = 0.74$ mm). Note that in Figure 8 there is virtually no difference between the ranges of q_s in the two samples because D does not appear in the definition of q_s .

Figure 7 is important, but in a sense it is misleading. The tight cluster of points on each graph is due in part to Δ and D appearing on both sides of Equation 18 – that is, there is spurious correlation. The scatter is greater in Figure 8 because there is no spurious correlation. Still, the scatter in Figure 8 is not excessive and, apart from the uppermost 10 points in Figure 8a, it is symmetrical around the line of perfect agreement. Considering the wide range of conditions represented by these data, this is a remarkable result.

The uppermost 10 points in Figures 7a and 8a all plot below the line of perfect agreement, signifying that Equation 18 consistently underpredicts the transport capacity of these flows. An inspection of the spreadsheets

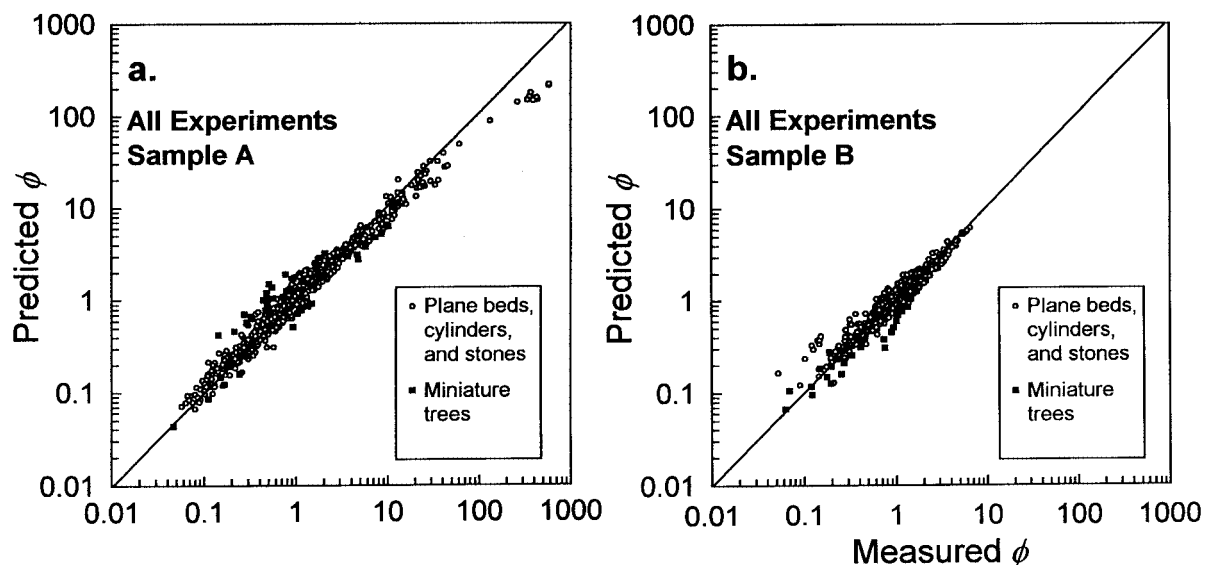


Figure 7. Graphs of ϕ predicted by Equation 18 against measured ϕ for all the experiments in samples A and B

discloses that not only do these flows have the highest transport capacities ($\phi > 200$ and $q_s > 0.0007 \text{ m}^2 \text{ s}^{-1}$) but they also have the highest sediment concentrations ($0.30 > C > 0.20$). In fact, these concentrations are so high that all 10 flows are probably hyperconcentrated (Costa, 1988; Pierson and Costa, 1987; Rickenmann, 1991). Further work is required to develop a sediment transport equation for hyperconcentrated flows and, in particular, for hyperconcentrated flows transporting well-sorted sediments.

Another interesting characteristic of these 10 flows is that they all occurred on stone-covered rather than plane beds. Furthermore, the stones on these beds were the largest ($D_r = 91.3 \text{ mm}$) and their concentrations were the highest ($0.57 \geq C_r \leq 0.24$) in the study. Evidently, stones of this size and concentration promote sediment transport by generating horseshoe vortices and concentrating the flow between the stones (Abrahams *et al.*, 2000). At the same time these stones inhibit sediment transport by obstructing the flow and reducing its velocity. Figure 5b suggests that in the case of the 10 hyperconcentrated flows in sample A, these two tendencies are in balance, as these flows plot closely around the line of perfect agreement for plane beds. It is not known whether this result is serendipitous or has some deeper meaning.

Additional tests

Abrahams *et al.* (2000) conducted six series of flume experiments aimed at elucidating the effect of stone cover and stone size on the transport capacity of interrill flow. The experiments were performed on two slopes (2° and 10°) with stones of three sizes D_r (28.0, 45.5 and 91.3 mm) serving as roughness elements. In all experiments the bed sediment diameter was 0.74 mm, the water inflow was $0.135 \times 10^{-3} \text{ m}^3 \text{ s}^{-1}$, and the rainfall intensity was 108 mm h^{-1} . In each series C_r varied from 0 to about 0.90. These data therefore provide an opportunity to test the model in general and Equations 18 to 20 in particular.

Figure 9 compares the measured values of ϕ with those predicted by the model for the three series of experiments on the 10° slope. The comparison is confined to the 10° slope because the flows in 90% of the experiments on this slope are turbulent (i.e. $Re > 5000$) as compared with 25% of the flows on the 2° slope. The agreement between measured and predicted values of ϕ is very good when D_r is 45.5 and 91.3 mm, but when $D_r = 28.0 \text{ mm}$ the model overpredicts ϕ at the highest values of C_r . This overprediction is attributed to progressive inundation of the 28-mm stones as h increases with C_r .

Overprediction probably occurs because in each experiment Q , u and C_r are measured and h is calculated assuming that $w = W(1 - C_r)$. However, as h increases with C_r , the flow spreads out over the stones and h increases more slowly than calculated. Because the positive effect of h on ϕ through $\theta^{1.5}$ ($\phi \propto h^{1.5}$) in

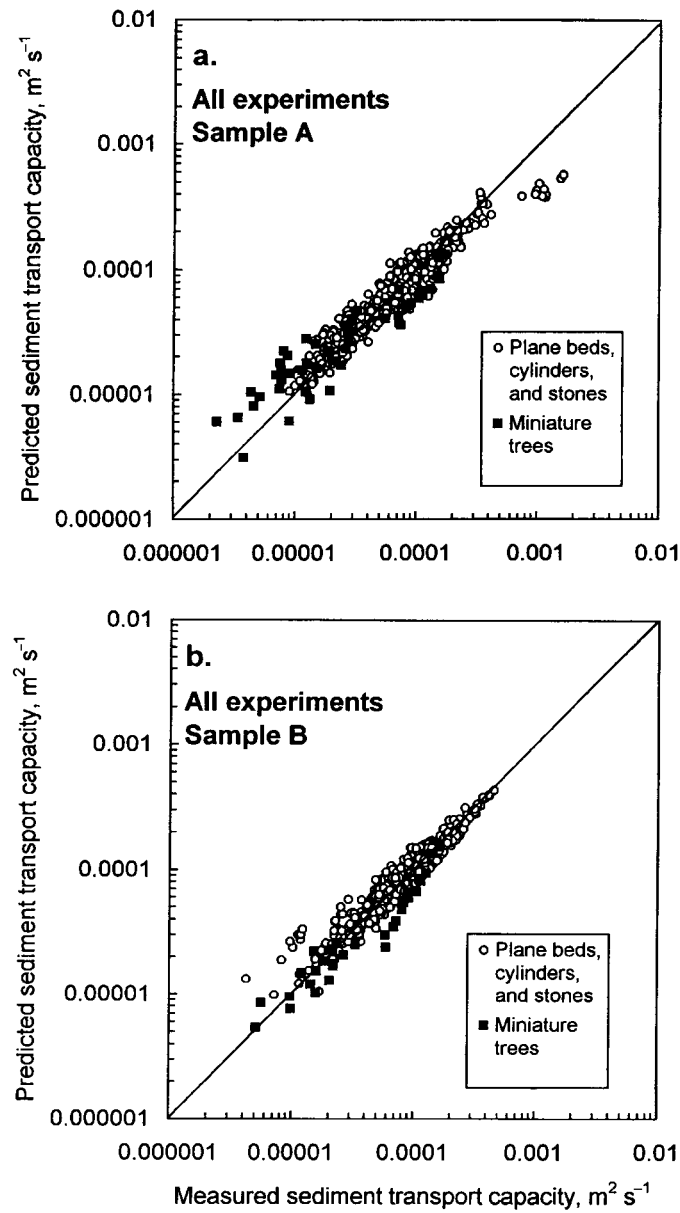


Figure 8. Graphs of sediment transport capacity predicted by Equation 18 against measured sediment transport capacity for all the experiments in samples A and B

Equation 18 is stronger than the negative effect through $(u/u_*)^{1-2} (\phi \propto h)^{0.5-1}$, the tendency for the model to overestimate h means that it also overestimates ϕ . Thus, inundation of the roughness elements needs to be taken into account when calculating the hydraulic variables in general and h in particular, otherwise ϕ will be overestimated.

CONCLUSION

The purpose of this study has been to derive a functional relationship that may be used to predict the sediment transport capacity of interrill overland flow. Such a relationship is difficult to develop because

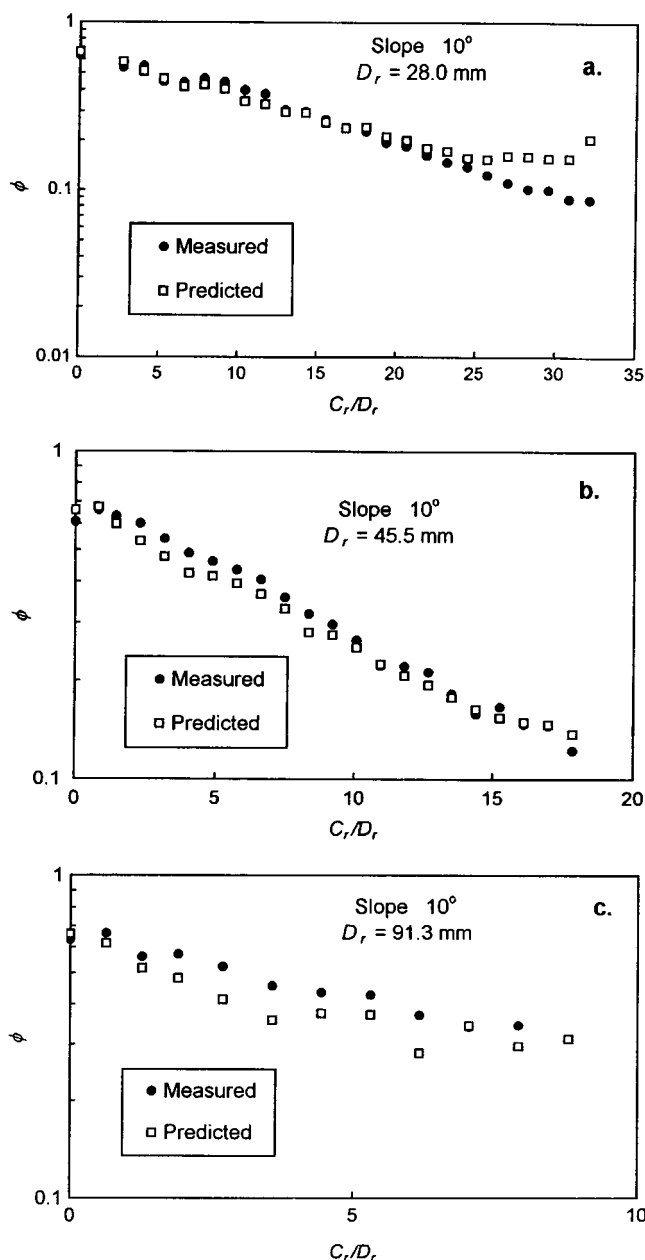


Figure 9. Graphs of ϕ predicted by Equation 18 and ϕ measured by Abrahams *et al.* (2000) against roughness concentration C_r . The three series of measurements were all made on a 10° slope with a water inflow of $0.135 \times 10^{-3} \text{ m}^3 \text{ s}^{-1}$ and a rainfall intensity of 108 mm h^{-1} . The roughness elements were stones with median roughness (cross-flume) diameters of (a) 28.0 mm (b) 45.5 mm and (c) 91.3 mm

interrill surfaces are hydraulically very rough and this roughness has an effect on transport capacity that is difficult to quantify. The approach adopted here has been to assume that the effect of surface roughness on transport capacity is largely captured by the flow hydraulics and to seek appropriate hydraulic variables to predict transport capacity. The transport of well-sorted non-cohesive sediments by turbulent flow on a plane bed is represented by 10 basic variables. Using dimensional analysis, these 10 variables are reduced to the dimensionless sediment transport rate ϕ and four dimensionless predictive variables θ , $1 - (\theta_c/\theta)$, u/u_* , and

w_i/u^* . The functional relationship has the form

$$\phi = a\theta^{1.5} \left(1 - \frac{\theta_c}{\theta}\right)^{3.4} \left(\frac{u}{u^*}\right)^c \left(\frac{w_i}{u^*}\right)^{-0.5}$$

where $\log a = -0.42 C_r/D_r^{0.20}$ and $c = 1 + 0.42 C_r/D_r^{0.20}$.

The model is parameterized using sample A which contains 649 flume experiments in which flow rate, rainfall rate, bed slope, sediment size, and roughness size, shape and concentration all vary widely. The model is tested using sample B, which is comparable to sample A except that it contains only one sediment size. In addition, the model is tested by comparing its predictions with the results of three series of experiments conducted by Abrahams *et al.* (2000). The tests confirm that the model gives good unbiased predictions of transport capacity when $C < 0.2$ but underpredicts transport capacity in hyperconcentrated flows when $C > 0.2$. Given the diverse shapes, sizes and concentrations of roughness elements in this study, the transport model is expected to apply to a broad range of ground surface morphologies.

It is evident from an inspection of the transport model that, although the predictive variables in the model are hydraulic, data on the concentration and size of the roughness elements are still required to calculate these variables. In addition, data are required on flow depth, velocity and discharge. In most applications, such data probably will be obtained from a rainfall–runoff model (possibly embedded within a soil erosion model). Care is urged in using such models because flow discharge and soil loss generally are computed per unit hillslope width, whereas flow discharge and transport capacity are calculated in the transport model per unit flow width.

Although only sand was used in the present experiments, several lines of evidence suggest that the transport model applies to a much wider range of sediments. First, the dimensional analysis is not restrictive insofar as it specifies only that the sediment be well sorted and non-cohesive. Second, the transport model is an extension of the total-load transport equation for open-channel flows (Equation 17), which has been shown to apply to sediments ranging from 0.17 to 23.5 mm in diameter (Figure 4). Third, because the transport model contains all the variables that affect the transport of bed sediments, including relative sediment density Δ , the model should apply not only to primary soil particles but to aggregates as well, provided they are non-cohesive. Additional work is needed to test this proposition.

ACKNOWLEDGEMENTS

This research was supported by the Geography and Regional Science and the Jornada Long-term Ecological Research (LTER) programmes of the National Science Foundation. We are grateful to Hassan Pourtaheri and Don Rankin for assistance in designing and constructing the flumes and to Maneesha Joshi, Mat Kramer, Scott Rayburg, Frank Aebly and Nathan Fischer for help in carrying out the experiments.

REFERENCES

- Abrahams AD, Parsons AJ. 1994. Hydraulics of interrill overland flow on stone-covered desert surfaces. *Catena* **23**: 111–140.
- Abrahams AD, Parsons AJ, Hirsch PJ. 1992. Field and laboratory studies of resistance to interrill overland flow on semi-arid hillslopes, southern Arizona. *Overland Flow: Hydraulics and Erosion Mechanics*, Parsons AJ, Abrahams AD (eds), UCL Press: London; 1–23.
- Abrahams AD, Li G, Krishnan C, Atkinson JF. 1998. Predicting sediment transport by interrill overland flow on rough surfaces. *Earth Surface Processes and Landforms* **23**: 1087–1099.
- Abrahams AD, Gao P, Aebly FA. 2000. Relation of sediment transport capacity to stone cover and size in rain-impacted interrill flow. *Earth Surface Processes and Landforms* **25**: 497–504.
- Atkinson JF, Abrahams AD, Krishnan C, Li G. 2000. Shear stress partitioning and sediment transport by overland flow. *Journal of Hydraulic Research* **38**: 37–40.
- Aziz NM, Scott DE. 1989. Experiments on sediment transport in shallow flows in high gradient channels. *Hydrological Sciences Journal* **34**: 465–478.
- Bagnold RA. 1966. *An Approach to the Sediment Transport Problem from General Physics*. Professional Paper 422-I, U.S. Geological Survey, Washington, DC.
- Bagnold RA. 1973. The nature of saltation and of 'bed-load' transport in water. *Proceedings of the Royal Society of London Series A* **332**: 473–504.
- Bunte K, Poesen JW. 1994. Effects of rock fragment size and cover on overland flow hydraulics, local turbulence and sediment yield on an erodible soil surface. *Earth Surface Processes and Landforms* **19**: 115–135.

- Chiew Y-M, Parker G. 1994. Incipient motion on non-horizontal slopes. *Journal of Hydraulic Research* **32**: 649–660.
- Costa JE. 1988. Rheologic, geomorphic, and sedimentologic differentiation of water floods, hyperconcentrated flows, and debris flows. In *Flood Geomorphology*, Baker VR, Kochel RC, Patton PC (eds). Wiley: New York; 113–122.
- Coussot P. 1997. *Mudflow Rheology and Dynamics*. Balkema: Rotterdam; 255 pp.
- Dunne T, Dietrich WE. 1980. Experimental investigation of Horton overland flow on tropical hillslopes: 2. Hydraulic characteristics and hillslope hydrographs. *Zeitschrift fur Geomorphologie Supplement Band* **35**: 60–80.
- Dunne T, Zhang W, Aubry BF. 1991. Effects of rainfall, vegetation, and microtopography on infiltration and runoff. *Water Resources Research* **27**: 2271–2286.
- Foster GR, Flanagan DC, Nearing MA, Lane LJ, Risse LM, Finkner SC. 1995. Hillslope erosion component. In *USDA-Water Erosion Prediction Project Hillslope Profile and Watershed Model Documentation*, NSERL Report 10, National Soil Erosion Research Laboratory: West Lafayette, IN; 11.1–11.12.
- Gao P. 2001. *Analysis of Bedload Transport in Saltation and Sheetflow Regimes*. PhD dissertation, State University of New York at Buffalo: Buffalo, NY.
- Gao P, Abrahams AD. (In review). Bedload transport resistance in rough open-channel flows. *Journal of Hydraulic Engineering*.
- Govers G. 1987. Initiation of motion in overland flow. *Sedimentology* **34**: 1157–1164.
- Govers G. 1992. Evaluation of transport capacity formulae for overland flow. In *Overland Flow: Hydraulics and Erosion Mechanics*, Parsons AJ, Abrahams AD (eds). UCL Press: London; 243–273.
- Govers G, Rauws G. 1986. Transport capacity of overland flow on plane and irregular beds. *Earth Surface Processes and Landforms* **11**: 515–524.
- Graf WH, Suszka L. 1987. Sediment transport in steep channels. *Journal of Hydroscience and Hydraulic Engineering* **5**: 11–26.
- Guy HP, Simons DB, Richardson EV. 1966. *Summary of Alluvial Channel Data From Flume Experiments, 1956–61*. Professional Paper 462-I, U.S. Geological Survey: Washington, DC.
- Hirsch PJ. 1996. *Hydraulic Resistance to Overland Flow on Semiarid Hillslopes: a Physical Simulation*. PhD dissertation, Department of Geography, State University of New York at Buffalo: Buffalo, NY; 154 pp.
- Kinnell PIA. 1973. The problem of assessing the erosive power of rainfall from meteorological observations. *Soil Science Society of America Proceedings* **37**: 617–621.
- Kirkby MJ, Abrahart R, McMahon MD, Shao J, Thornes JB. 1998. MEDALUS soil erosion models for global change. *Geomorphology* **24**: 35–49.
- Lawrence DSL. 2000. Hydraulic resistance in overland flow during partial and marginal surface inundation: experimental observations and modeling. *Water Resources Research* **36**: 2381–2393.
- Leeder MR. 1982. *Sedimentology: Process and Product*. George Allen and Unwin: London; 344 pp.
- Li G, Abrahams AD. 1997. Effect of saltating sediment load on the determination of the mean velocity of overland flow. *Water Resources Research* **33**: 341–347.
- Li G, Abrahams AD. 1999. Controls of sediment transport capacity in laminar interrill flow on stone-covered surfaces. *Water Resources Research* **35**: 305–310.
- Miller MC, McCave IN, Komar PD. 1977. Threshold of sediment motion under unidirectional currents. *Sedimentology* **24**: 507–527.
- Morgan RPC, Quinton JN, Smith RE, Govers G, Poesen JWA, Auerswald K, Chisci G, Torri D, Styczen ME. 1998. The European soil erosion model (EUROSEM): a dynamic approach for predicting sediment transport from fields and small catchments. *Earth Surface Processes and Landforms* **23**: 527–544.
- Nnadi FN, Wilson KC. 1992. Motion of contact-load particles at high shear stress. *Journal of Hydraulic Engineering* **118**: 1670–1684.
- Owen WM. 1954. Laminar to turbulent flow in a wide open channel. *Transactions of the American Society of Civil Engineers* **119**: 1157–1164.
- Pierson TC, Costa JE. 1987. A rheological classification of subaerial sediment-water flows. *Reviews in Engineering Geology*, Vol. III. Geological Society of America: Boulder, CO; 1–12.
- Rickenmann D. 1991. Hyperconcentrated flow and sediment transport at steep slopes. *Journal of Hydraulic Engineering* **117**: 1419–1439.
- Savat J. 1980. Resistance to flow in rough supercritical sheet flow. *Earth Surface Processes* **5**: 103–122.
- Schoklitsch A. 1914. *Über Schleppekraft und Geschibebewegung*. Engelmann: Leipzig.
- Smart GM. 1984. Sediment transport formula for steep channels. *Journal of Hydraulic Engineering* **110**: 267–276.
- Smith RE, Goodrich DC, Woolhiser DA, Unkrich CL. 1995. KINEROS – a kinematic runoff and erosion model. In *Computer Models of Watershed Hydrology*, Singh VP (ed.). Water Resources Publications: Highlands Ranch, CO; 697–732.
- Song T, Chiew YM, Chin CO. 1998. Effect of bed-load movement on flow friction factor. *Journal of Hydraulic Engineering* **124**: 165–175.
- Stevens MA, Simons DB, Lewis GL. 1976. Safety factors for rip-rap protection. *Journal of the Hydraulics Division, Proceedings of the American Society of Civil Engineers* **102**: 637–655.
- Straub LG. 1939. Studies of the transition-region between laminar and turbulent flow in open channels. *Transactions of the American Geophysical Union* **7**: 649–653.
- Van Rijn LC. 1993. *Principles of Sediment Transport in Rivers, Estuaries and Coastal Seas*. Aqua Publications: Amsterdam.
- Williams GP. 1970. *Flume Width and Water Depth Effects in Sediment-transport Experiments*. Professional Paper 562-H, U.S. Geological Survey: Washington, DC.
- Woo D-C, Brater EF. 1961. Laminar flow in rough rectangular channels. *Journal of Geophysical Research* **66**: 4207–4217.
- Yalin MS. 1972. *Mechanics of Sediment Transport*. Pergamon Press: New York; 298 pp.